Humeral tissue remodeling in contact with pyrocarbon interposition implant

Rémy Gauthier, G. Ouenzerfi, I. de Gaudemaris, N. Attik, A. Godenèche, J. Garret, R. Gravier, M. Hassler, A.-M. Trunfio-Sfarghi, P. Boileau

Humeral tissue remodeling in contact with pyrocarbon interposition implant

R.Gauthier[a], G.Ouenzerfi[b], I.de Gaudemaris[c], N.Attik[d], A.Godenèche[e], J.Garret[f], R.Gravier[g], M.Hassler[b], A-M. Trunfio-Sfarghi[c], P.Boileau[h]

[a] Univ Lyon, CNRS, INSA Lyon, UCBL, MATEIS, UMR5510, F-69621 Villeurbanne, France

[b] Tornier SAS, Grenoble, France

[c] Univ Lyon, CNRS UMR5259, INSA-Lyon, LaMCoS, Villeurbanne F-69621, France

[d] Univ Lyon, Université Claude Bernard Lyon 1, UMR CNRS 5615, Laboratoire des Multimatériaux et Interfaces, F-69622 Villeurbanne, France

[e] Hôpital Privé J Mermoz Ramsay-GDS-Centre orthopédique Santy, Lyon, France

[f] Clinique du Parc, Lyon, France

[g] Institut de la main et du membre supérieur, Marseille, France

[h] ICR Institut de chirurgie Réparatrice. 7, avenue Durante 06000 Nice, France

Corresponding author: Rémy Gauthier, 7 avenue Jean Capelle, Bâtiment Blaise Pascal, Laboratoire MatéIS UMR 5510, Villeurbanne Cedex 69621, France, remy.gauthier@cnrs.fr

Abstract

The interactions between pyrocarbon (PyC) interposition implants and human humeral cancellous bone leads to the formation of a new interpositional tissue made a dense layer of cortical bone and a cartilage-like tissue. A sample of the tissue in contact with the PyC interposition implant was harvested on the humeral bone side from 6 patients undergoing a re-operation for implant removal due to staged surgery or clinical failure related to pain. The samples where then prepared for histology to evaluate the tissue morphology and immunohistology to assess for the presence of collagen I and collagen II within the matrix. For all the cases, a layer of dense cortical bone and a layer of soft tissue was observed between the PyC interpositional implant and the humeral cancellous bone. The nature of the interpositional soft tissue was different between the cases. While the hypothesis that a new tissue was modelled at PyC - humeral cancellous bone interface was confirmed, the nature of the soft interpositional tissue evolved from a fibrocellular to a cartilage-like tissue depending on the cases. The hypotheses for the different nature of the soft interpositional tissue observed between the different cases was based on humeral bone mechanobiological remodeling. The influence of the degree of attachment between the soft and bony interpositional-tissues and on the PISA geometry on the soft interpositional tissue nature are discussed. Further

investigations on the role of humeral bone and on the PISA biomechanics should be performed to better understand this tissue remodeling.

Keywords: Pyrocarbon interposition shoulder arthroplasty, tissue remodeling, mechanobiology, bone-implant interactions

1 Introduction

Basically, there are two types of anatomical shoulder replacements: total shoulder arthroplasty (TSA) or hemi-arthroplasty (HA). While TSA leads to good outcomes when considering short terms clinical results. High rates of the glenoid component failure have been reported at mid and long term follow up in young patients under 60 years [1,2]. On the other hand, 75 % of patients undergoing HA procedure are experiencing shoulder pain due to the glenoid wear in a 17-years follow-up clinical study [3]. Consequently, TSA and HA may not be relevant procedures for younger patients with–glenohumeral osteoarthritis and other innovative solutions are currently explored.

In that context, some current research works are focused on the use of interposition implants. Historically, soft tissues (tendons or ligaments) have been first used as interposition arthroplasties to reconstruct destroyed articulations like the elbow [4]. More recently, spherical Pyrocarbon (PyC) implants have been proposed in hand and wrist reconstructive surgery and now in shoulder surgery reconstruction [5]. Promising results are explained through PyC capacity to induce little damage to bone and cartilage [6,7]. HA using PyC resurfacing implant are also applied [8]. Still, abnormal implant fractures after a HA using a PyC resurfacing implant have been explained by the too low mechanical properties of the PyC to allow for the implant impaction [9,10]. This warrants PyC interposition shoulder arthroplasty (PISA), using spherical PyC implant, to be considered as a relevant healing strategy [11]. Pyrocarbon interposition implant is interesting, due to its spherical shape, its elastic modulus close to cortical bone's apparent modulus [12,13], and its capacity not to adhere to the native bone. Together, these properties have promoted the formation and remodeling of an interpositional-tissue, or interpositional tissue, at the interface between the PyC implant and humeral bone for the 6 cases investigated. To the authors, this is the first time such a tissue is observed at the interface between human bone and a spherical implant. Still, investigating tissues remodeling in contact with PyC is determinant to understand PISA clinical outcomes. While the reaction of sclerotic bone (like the one of the glenoid surface) is partially known, the reaction of pure cancellous bone in contact with a spherical PyC implant is totally unknown.

The purpose of the present study was to perform histologic analysis of the membrane of humeral bone tissue in contact with pyrocarbon interposition implants. The tissue was

harvested in six shoulders of patients re-operated for implant removal in the context of staged surgery (in case of previous infection) or in case of clinical failure related to shoulder pain. We hypothesized that the cancellous bone would resist to loads of the PISA by forming a layer of cortical bone and that some cartilage-like tissue would be found directly in contact with the PISA.

2 Materials and methods

2.1 Cohort

The cohort of the present study consists in 6 patients (Table 1), a revision surgery after a PyC interposition implant arthroplasty was performed between 2013 and 2021 in 4 French different medical centers (Clinique Mermoz, Lyon; Clinique du parc, Lyon; Clinique Monticelli-Vélodrome, Marseille; Hôpital Pasteur 2, Nice). The patients needed surgery revision for different reason, summarized in **Erreur ! Source du renvoi introuvable.**. The functional reason signifies that the patient had diminished mobility or suffered from pain. On the other end, 2 patients from the cohort had undergone a PISA as surgical treatment to treat shoulder infection, the PyC implant being u>sed as temporary spacer [14]. For those patients, the revision surgery occurred while no functional issue was claimed.

Figure 1: Case 2 right shoulder radiography before revision surgery.

The pyrocarbon interposition implant has been placed using standards procedures [6,15]. An important point is that the humeral head has been removed, and a cavity has been drilled in the humeral bone to the spherical pyrocarbon implant to lodge (Figure 1). Spherical reaming of the proximal humerus is needed to implant the PISA; the reamer must have the same diameter than the definitive implant for perfect congruence between the humeral cavity and the implant. On this radiographic image, one can notice the dense and circular line of cortical bone and the clear space between the humeral bone and the spherical PyC implant, which corresponds to the new formed tissue. Such qualitative morphology was observed for all the clinical cases.

2.2 Interpositional-tissue dissection

During the revision surgery, the surgeons have observed that a new tissue had been synthetized at the interface between pyrocarbon implants and humeral bone (Figure 2). The appearance and handling of this interpositional-tissue was not the same between the different patients. The neo tissue formed in the humeral cavity of case 1 was easily harvested. Macroscopically, this interpositional-tissue appears as a meniscus-like tissue between the bone and the implant, with some attachment sites to the synovial membrane. The

interpositional-tissue was removed from cases 2 and 3 by the surgeon without damaging it. For these cases, the interpositional-tissue could be easily removed from the humeral cavity (Figure 2). By contrast, the tissue in cases 4 and 5 was thin (less than 1 mm) was hardly removed from the humeral bone. In that manner, the samples have been largely damaged during the harvest operation. The interpositional-tissue formed in clinical case 6 was firmly bonded to bone. It has hence been asked to the surgeon to remove a core sample of both the bonded tissue and bone for further analyses. It should be noticed that the interpositional-tissue was never bonded to the pyrocarbon implant surface. In table 1, the Walch classification is associated with the glenoid erosion state in the case of glenohumeral osteoarthritis [16]. This thus provide information on the geometry of the glenoid cavity. The tissue samples were recovered with the patients and the surgeons' consent.

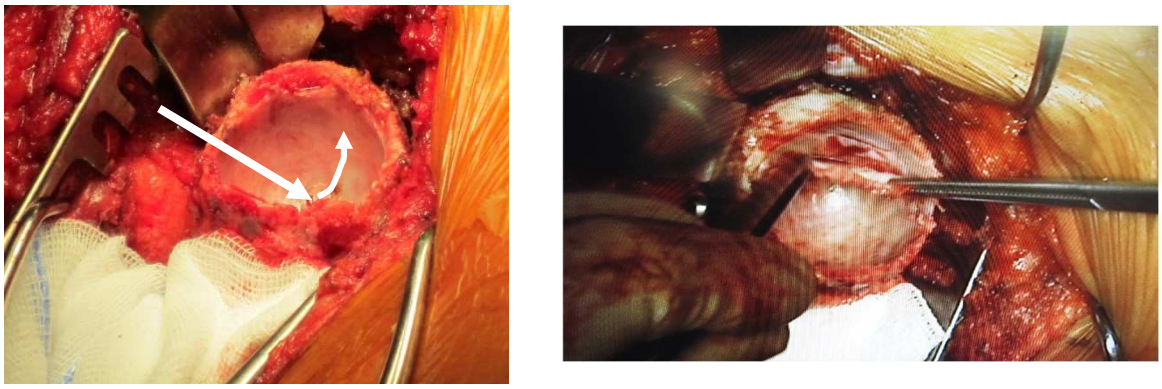

Figure 2 Left: photograph of the interpositional-tissue on the humeral cavity of clinical case 3 before its removal. Right: photograph showing that to remove this interpositional-tissue, the surgeon has to pull it out from the bone, while it has been classified as being only slightly bonded to humeral bone. The interpositional-tissue membrane has been harvested at the center of then cavity, shown by the straight arrow, and toward the border of the cavity, as shown by the curved arrow.

Table 1 Summary of the cohort clinical data

Cases	Sexe	Age (years)	Surgeon*	Implanted time (Months)	Implant diameter (mm)	Walch classification of glenoid morphology before PISA	Indication for PISA	Reason for revision
1	♂	74	PB	6	44	NA	Sepsis on RSA	Temporary spacer
2	♂	78	AG	6	36	NA	Sepsis due to previous surgery	Temporary spacer
3	♀	52	JG	25	32	C	Osteoarthritis due to a brachial plexus paralysis	Small diameter and glenoid dysplasia induced a humeral translation
4	♂	-	JG	31	42	B1	To avoid the placement of a glenoid implant	Pain due to a conflict between calcar and glenoid
5	♀	60	AG	60	34	A1	Post-traumatic osteoarthritis	Pain due to a conflict between calcar and glenoid
6	♂	60	RG	5	46	NA	RSA loosening with suspected infection	Temporary spacer

** : PB : P.Boileau, AG : A.Godenèche, HG : H.Garret, RG : R.Gravier. NA = Non Applicable*

2.3 Interpositional-tissue analyses

Once harvested, the samples were placed in a sterile container and sent back to Lyon. Samples were fixed in ROTI®Histofix 4 %, 4 % formaldehyde, ready-to-use, phosphate buffered, pH 7 for 24h before being decalcified for 7h (PEURDO, Eurobio, France). The samples were then dehydrated using successive bath of ethanol, acetone, and xylene, and embedded in paraffin. The samples were embedded so as bone and implant sides of the interpositional-tissue can be easily identified.

Different sections of 5 µm were then cut from the embedded samples. After removing the paraffin, Hematoxylin, Eosin, Safran (HES) staining was applied on different sections. HES stains cells nuclei in purple, cells cytoplasm in pink, and extracellular matrix (ECM) in yellow.

In addition, immunohistochemical stainings have been applied on 5 µm sections for cases 1, 2, and 5. After removing the paraffin, each section has been immerged in 0.5 % hyaluronidase buffered in PBS-BSA 3% for 1h at room temperature, in order to expose the antigenic sites. Sections were then incubated with rabbit anti-human type I collagen (Coll I) antibody diluted at 1/1000 (Novotec, 20111), rabbit anti-human type II collagen (Coll II) antibody diluted at 1/500 (Novotec, 20211) overnight at 4 °C buffered in PBS-BSA 3%. Sections are then incubated with goat anti-rabbit secondary anti-body coupled with peroxidase (Dako, Envision Lapin, réf. K4002). A further reaction with diaminobenzidine (Dako, K3468) reveals the antigenic – antibody complexes through a brown color. Negative controls were prepared using a solution of PBS-BSA 3% instead of the primary antibodies.

The sample preparation and analysis from case 6 were performed by the Ciqle platform (Lyon, France). Samples preparations and analyses from the other cases were performed by Novotec (Lyon, France).

3 Results

All the cases showed radiographical evidence for the formation of a dense cortical layer and a soft layer formed between humeral cancellous bone and the PyC implant (Figure 1). In the framework of the current study, we will mainly focus on the soft interpositional-tissue near the center of the joint, where the loading occurs.

3.1 Case 1

The interpositional-tissue modeled at the bone-implant interface of clinical case 1 formed a dense membrane, from 3 mm to 1 mm in width in the cavity border and cavity center sides, respectively. The thin dense fibrocellular layer is clearly observed (→). Vascular canals (*) were observed, mostly on the bone side (Figure 3).

The HES staining showed that this interpositional-tissue was highly cellularized. The cell population was dominated by fibroblastic-type cells (Figure 4).

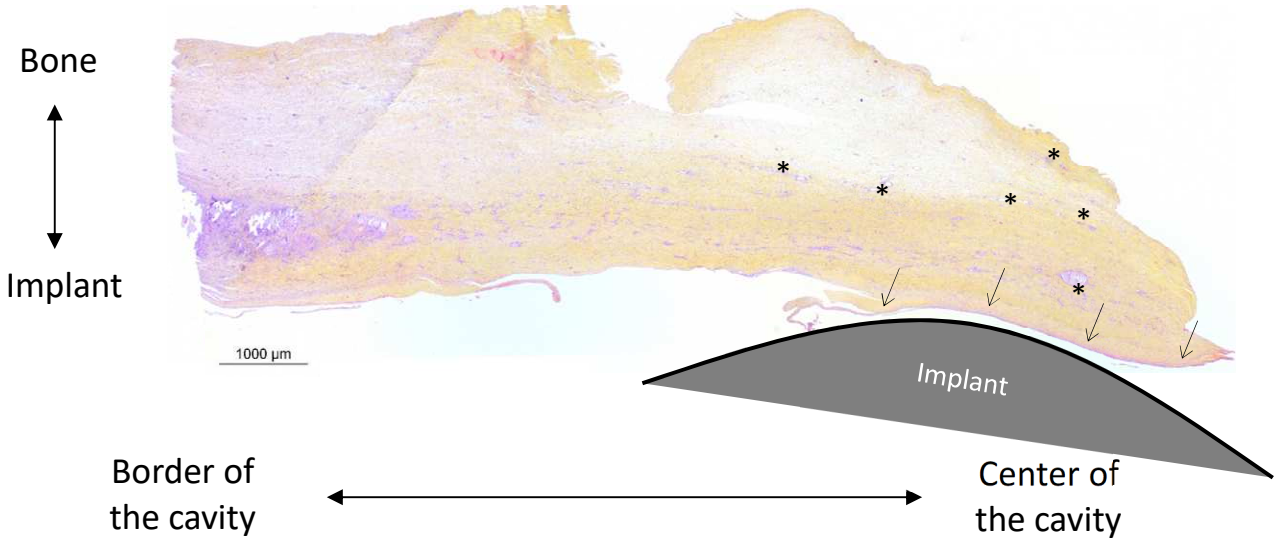

*Figure 3 Overall view of the interpositional-tissue synthetized at case 1 bone-implant interface (HES staining). * identifies the vascular canals. → identifies the dense layer. The implant illustration is not to scale.*

The immunostaining has revealed a homogeneous presence of Coll I, whereas Coll II were heterogeneously dispersed within the ECM. The interpositional-tissue is formed of both dense fibrillar and fibrocellular matrices made of Coll I. Vascular canals are observed on the bone side (Figure 4).

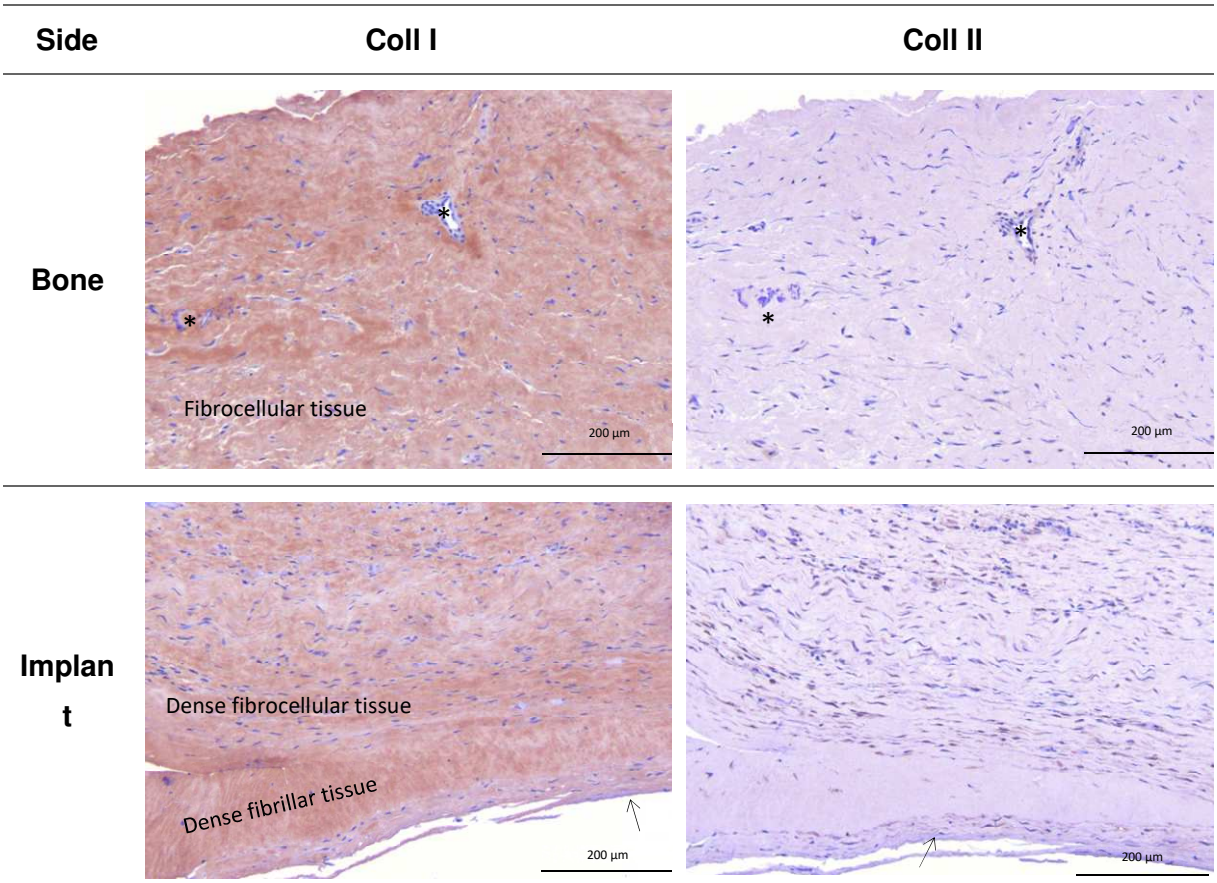

*Figure 4 Coll I and Coll II immunostainings of interpositional-tissue from clinical case 1 at the bone (top) and implant (bottom) sides. * identifies the vascular canals. → identifies the external thin dense layer.*

3.2 Case 2 and case 3

For case 2 and 3, the interpositional-tissue was a dense membrane, 1 mm or less in width toward the cavity center. The thin dense layer (→) at the implant side is less dense in cells that in the previous case. Highly vascularized (*) areas toward the bone are observed. In the interpositional-tissue formed at the bone implant interface of case 3, a large amount of adipose tissue is observed toward the cavity border (Figure 5).

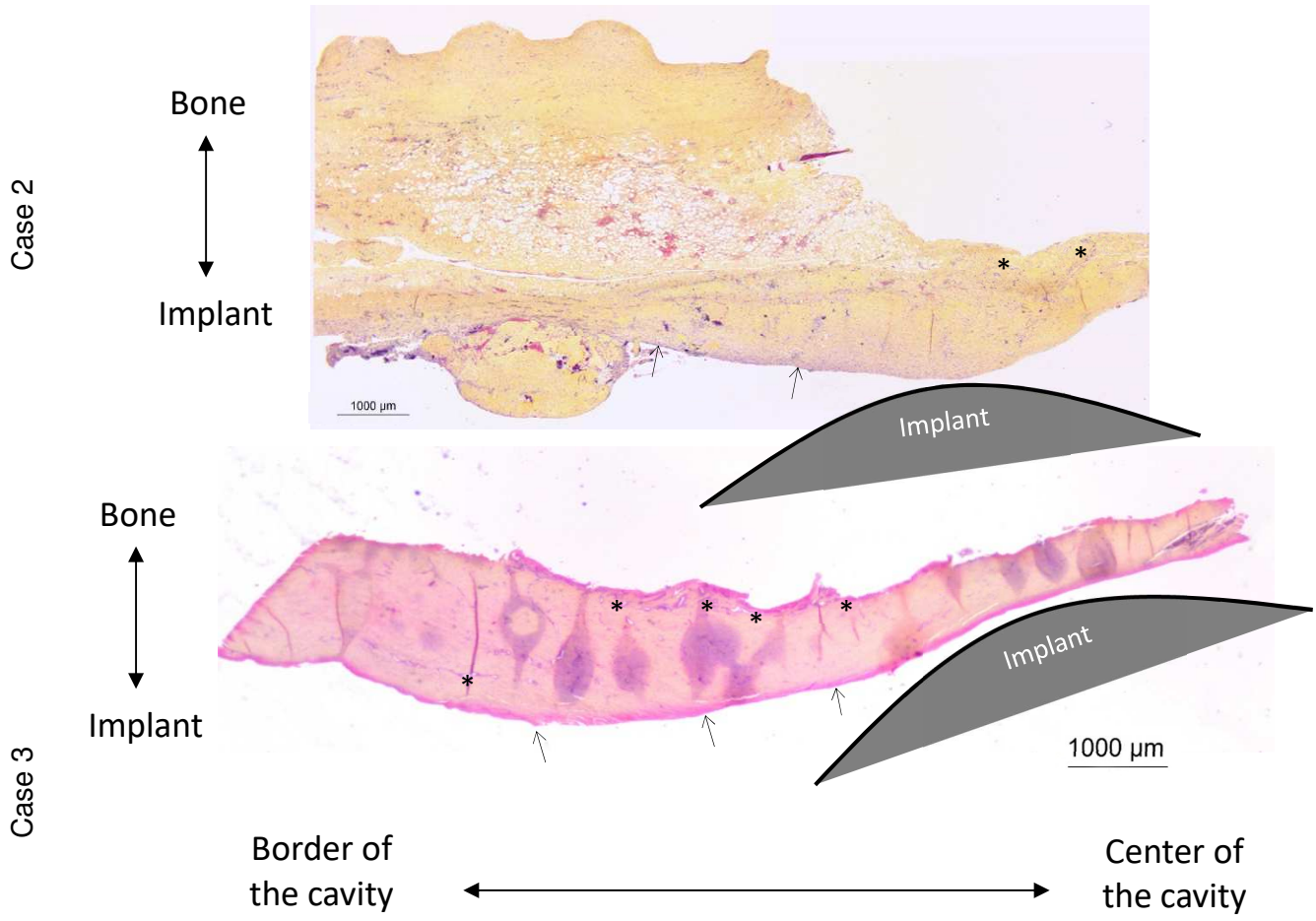

*Figure 5: Overall view of the interpositional-tissue synthetized at case 2 (top) and 3 (bottom) bone-implant interface (HES staining). * identifies the vascular canals. → identifies the dense layer. The implant illustrations are not to scale.*

Coll I immunostaining showed that the interpositional-tissue is formed of a heterogeneous matrix, with both fibrillar and fibrocellular tissues. The cells population is mainly fibroblastic. In contrast with the previous case, Coll II is expressed near the bone surface. Immunostainings showed Coll I and Coll II markers both in the ECM and intracellularly by the chondroblast-like cells (►). Intracellular Coll II is more intensively present than intracellular Coll I. Intracellular Coll II is more present in the implant side compared to the bone side.

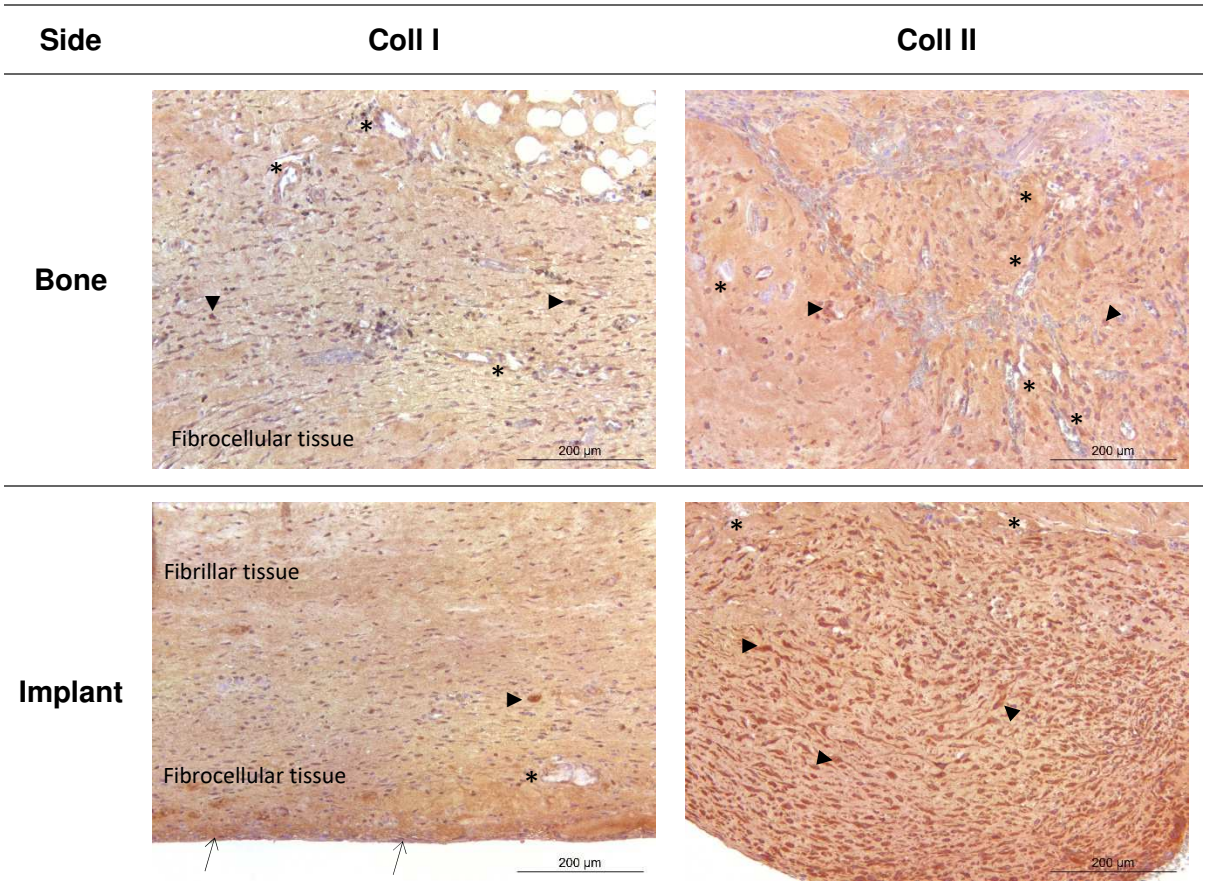

*Figure 6 Coll I and Coll II immunostainings of interpositional-tissue from clinical case 3 at the bone (top) and implant (bottom) sides. * identifies the vascular canals. → identifies the external thin dense layer. ► identifies the intracellular Col I and Coll II.*

3.3 Case 4 and case 5

These two samples had to be scratch out from the humeral cavity by the surgeon. This resulted in damaged samples that have been folded during the preparation process. In that case, the bone / implant sides, or the cavity border / cavity center sides were difficult to define. Still, some bone pieces can be observed. It is worth noticing the presence chondrocyte-like cells (O) rounded cells located in lacunae within the ECM, (Figure 7).

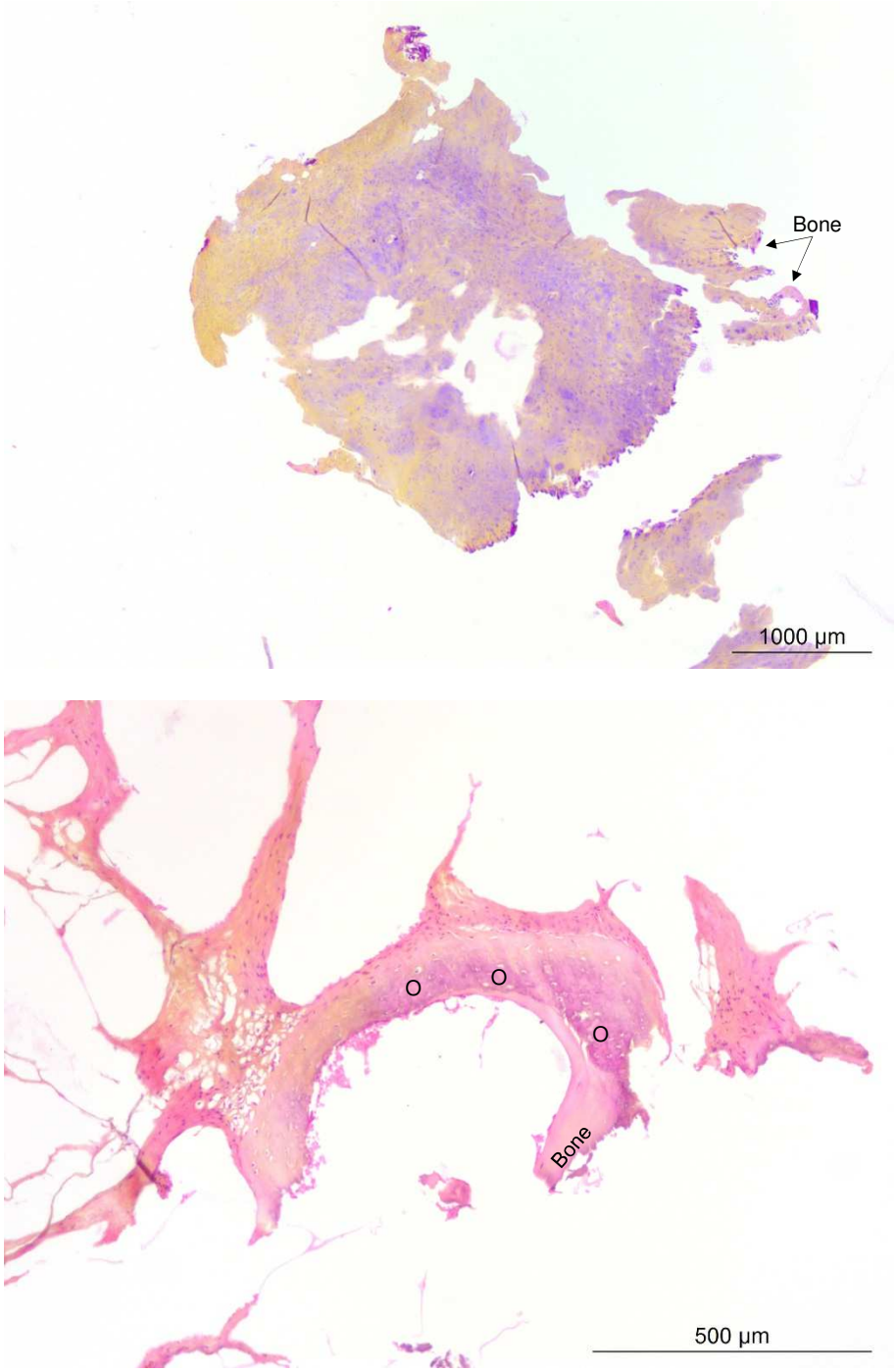

Figure 7 Overall view of the interpositional-tissue synthetized at case 4 (top) and 5 (bottom) bone-implant interface (HES staining). O identifies chondroblast cell populations. It has to be noticed that the scales between case 4 (top) and case 5 (bottom) are different. For these cases, the samples were too much damages during the preparation process and the implant and bones sides could not been identified.

Coll I and Coll II immunostainings show a thin layer of dense tissue that looks like the external dense layer observed at the implant side for the previous cases (→). Coll I immunostaining appeared less intense than for the previous cases. Still, some areas of dense Coll I are observed. Coll II is present intracellularly within rounded chondroblast-like cells (►). A large population of chondrocyte-like cells is observed. Fibroblast-like cells are also observed. Coll II is observed around vascular canals (**) (Figure 8).

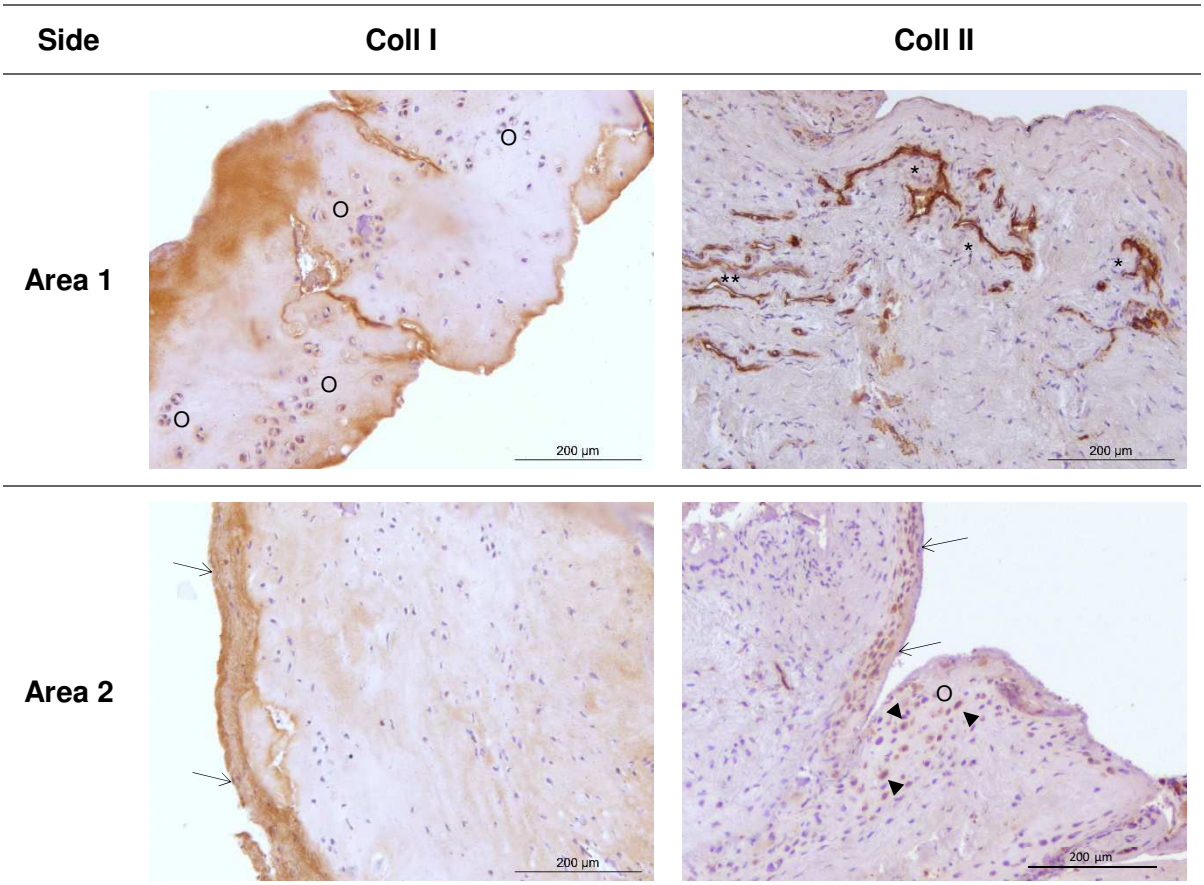

*Figure 8 Coll I and Coll II immunostainings of interpositional-tissue from clinical case 5 in different areas (area do not corroborate between Coll I Coll II immunostainings). * identifies the vascular canals. → identifies a thin dense layer that looks like the thin dense external layer. ► identifies the intracellular Coll II. For these cases, the samples were too much damages during the preparation process and the implant and bones sides could not been identified.*

3.4 Case 6

The interpositional-tissue of case 6 was firmly bonded to the humeral bone, making it impossible for the surgeon to harvest it without damaging it. The surgeon was then asked to harvest a core of both bone and interpositional-tissue. The dense bone on the upper side can clearly be observed and identify. Close to the interface with the soft interpositional-tissue, some small porosities (50 – 100 µm in diameter) that widen as we go further from this interface. This reminds the cortical layer and trabecular bone present in joint subchondral bones. The sample showed a dense interpositional-tissue, forming a 2 mm width membrane. The core extraction technique used by the surgeon allowed to observe the firm bonds between the humeral bone and the interpositional-tissue. The vascular canals are clearly observed on the bone side whereas no canal (*) is observed on the implant side. The cell population showed by the HES staining is mainly chondroblast-like. Close to this interface, some cells alignments were observed ([). Some cells clusters by two (●●) or more (●●●) were also observed, reminding cartilage isogenous groups [17]. Clusters of several cells were organized in circle and found close to the implant interface. Fibers from the interpositional-tissue appear to be inserted within

the more mineralized tissue (┬). Some amorphous cartilaginous matrix is also observed, reminding of articular cartilage. A tidemark I is present between an amorphous matrix and a bony matrix. Finally, a density gradient is observed from the interpositional-tissue toward the bone.

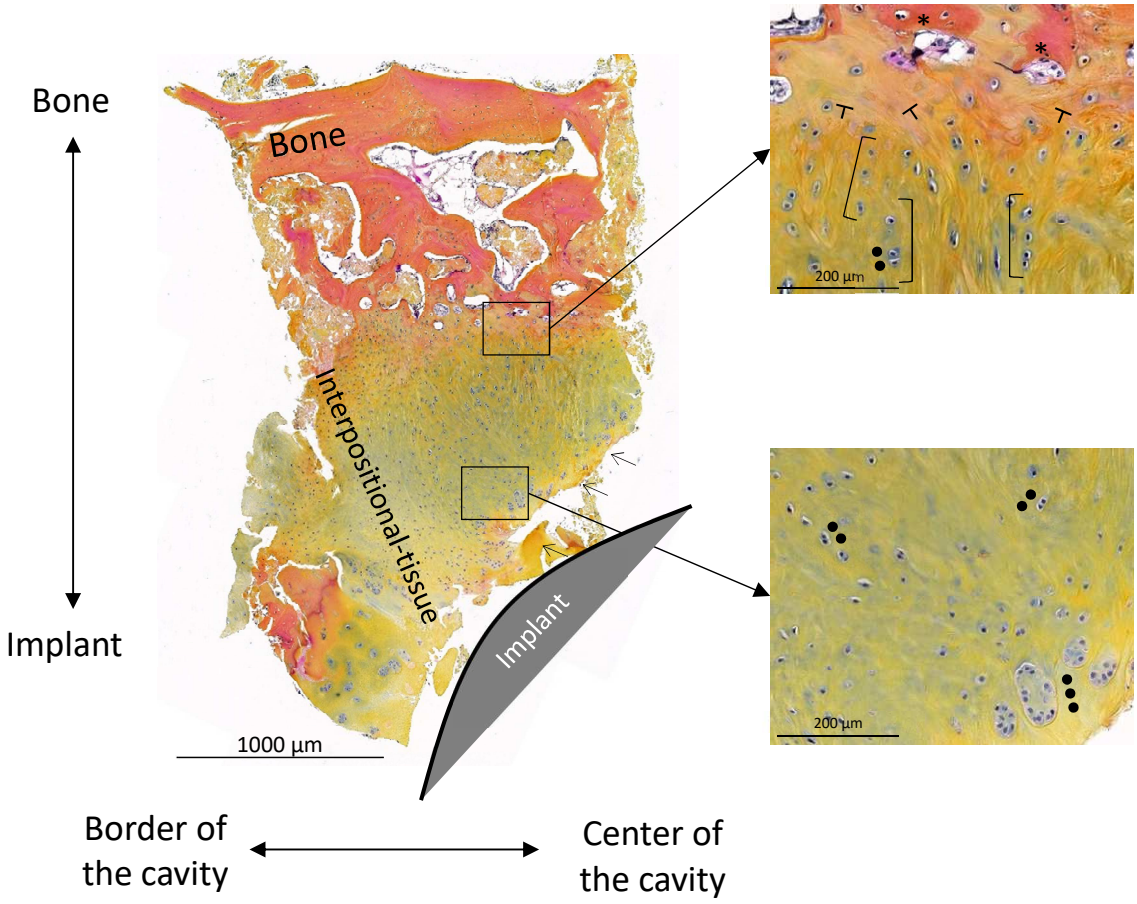

Figure 9 Overall view of the interpositional-tissue synthetized at case 6 bone-implant interface (HES staining). identifies the vascular canals. [identifies cells alignment close to the bone surface. ●● and ●●● identify the isogenic groups of 2 or more cells, respectively. ┬ identifies the interpositional-tissue fiber insertion sites in bone. TM: Tidemark. → identifies the external thin dense layer. The implant illustration is not to scale.*

Coll II immunostaining was much more expressed than Coll I at both bone and implant sides of the interpositional-tissue. There was a defined interface between bone and the interpositional-tissue at which Coll II was no more expressed. Still, some Coll II was observed within the bone away from this interface. Coll II was also observed around the vascular canals. Close to the implant side, Coll II immunostaining showed an amorphous ECM (Figure 10).

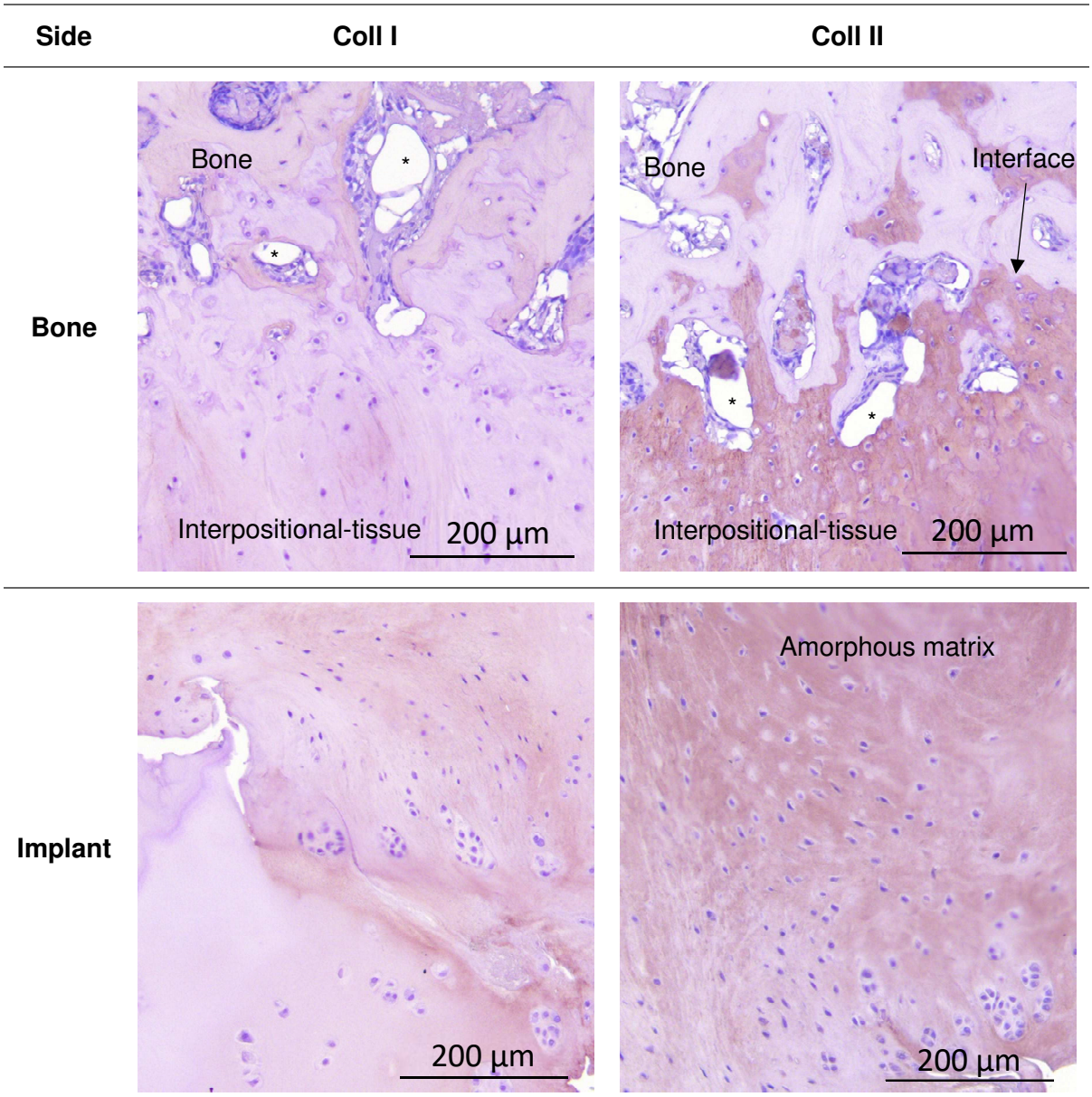

*Figure 10 Coll I and Coll II immunostainings of interpositional-tissue from clinical case 6 at the bone (top) and implant (bottom) sides. * identifies the vascular canals.*

4 Discussion

The results of the present study confirm our hypothesis: for some cases, a layer of cortical bone and some cartilage-like tissue can be observed at the interface between the cancellous bone of the proximal humerus and a spherical pyrocarbon interposition implant.

The nature of this interpositional-tissue differs between the different cases. In the results section, these 6 cases were organized in order to follow the evolution of the interpositional-tissue: from a non-cartilaginous (case 1) to the better cartilaginous tissue (case 6). With only six cases with different clinical data, the reason for these differences cannot be defined accurately. Still, some parameters known has being part in tissue modeling can be highlighted.

A parameter involved in the course of this interpositional-tissue remodeling can rely on the biomechanical conditions of the humeral bone - PyC implant system. The congruency between the implant and the humeral bone has a determinant influence on the load transmission between the PyC spherical implant and the bone. Such congruency depends on the implant diameter, the reaming of the humeral cavity and the glenoid cavity morphology based on their Walch classification. Additionally, it was interesting to notice that different binding degree between the interpositional-tissue membrane and the underlying bone was qualitatively observed. As an example, in case 1, the membrane of tissue was easily removed from the bone whereas a core was harvested from case 6. Such parameter is also involved in the distribution of the mechanical stresses transmitted to the underlying humeral bone. The degree of binding between bone and the interpositional-tissue influences mechanical loads transmission from the implant toward the humeral bone. While loose bonds allow from slight movements of the interpositional-tissue against humeral bone surface, firm bonds prevent from any relative movement. Load transmission between the interpositional-tissue and the underlying bone is thus better in the case of firm bonds.

Tissue differentiation at the bone implant interface highly depends on the mechanical loads transmitted to the cells lying in between the bone and the implant[18]. According to Prendergast et al., the nature of tissue differentiation at the bone implant interface depends on the strain experienced by the ECM, and the fluid velocity surrounding the cells [18]. In that context, PyC interposition implants have interesting properties compared to the general class of articular implants: they are not anchored within bone diaphysis, and they do not adhere to bone tissue. This results in a unique mechanical environment at the interface between humeral bone and the implant. During the patients' movement, the implant is able to glide on the humeral bone surface in a way that looks like humeral head movements within the glenoid[19]. The non-adhesive nature of PyC involves a continuous movement between the bone and the implant that prevent from bone formation between them. Instead, due to the shear strain induced by the implant movement, whether a fibrous or cartilaginous tissue will be synthetized [18]. Furthermore, the contact pressure distribution and the sliding speed between the implant and the native tissue are also known to influence the joint behavior by tuning the lubrication mode [20]. Still, the clinical data obtained in the framework of the current study do not allow to estimate such biomechanical parameters. Further investigation using 3D geometrical data might be of great interest to better understand the implanted joint biomechanics.

The load transmission from the PyC implant toward bone is of great importance, as it is believed that bone underlying the cartilage plays a major role in cartilage integrity [21]. Firm bonds hence may promote the mineralization of the interpositional-tissue and bone growth through a strain-guided mineralization mechanism [22], while loose bonds may promote the

development of a fibrous tissue [18]. This is in accordance with what has been observed in the current study, with the development of a real cartilage-like bone with the higher bone binding degree on case 6.

In this regard, investigating the distribution of contact points and pressured between the implant and the bone cavity might be of tremendous importance to understand the interpositional-tissue remodeling. Similarly, studying how and why such bonds between the interpositional-tissue and bone appear may help understanding this interpositional-tissue formation and appears as necessary to further control a suitable remodeling. Interestingly, the behavior of bone insertion sites is intensively investigated in the fields of tendon and ligament regeneration, where entheses play a major role [23]. Interestingly, the interpositional-tissue bone interface shown in Figure 9 presents similar features as cartilaginous entheses, with a gradient of tissue mineralization and fibers insertion sites [24], and cells alignment close to the bone interface [25]. In addition, the increasing content of Coll II in case 6 with a high bonding degree with bone is a marker of hyaline cartilage formation [26,27]. The presence and colocalization of both Coll I and Coll II suggest that this interpositional-tissue looks like articular cartilage, with characteristics of both fibro- and hyaline cartilage.

It is important to notice that such hypothesis might be considered for best cases, where the interpositional-tissue formed is adapted to optimal loads transmission. Still, as observed within the current study, this interpositional-tissue can evolve into a fibrocellular tissue that may not be suitable and may lead to disfunctions. Such fibrosis, highlighted by the presence of fibrillar matrix and a fibroblast-like cells population, may be associated with an inflammation of the synovial membrane [28,29]. Due to an abnormal function of the joint, the synoviocytes found in the synovial membrane may react by producing inflammatory factors that finally result in the formation of a fibrous tissue. Thus, the evolution of the properties of this interpositional-tissue lies in a close competition between fibrosis from synovial inflammation and mechanotransduction to the underlying humeral bone. Additionally, the degree of osteoporosis of the proximal humerus, the age and gender of the patients, the initial diagnosis (Primary OA, or fracture sequelae or infection…) are parameters that might be involved in the quality of the formation of the interpositional-tissue. In that context, in might be of great interests to closely investigate the structure and properties of the new formed interpositional cortical bone, down to the lacunocanalicular scale. The implant properties of the implant and the nature of the implant – bone interactions are known to influence osteocytes activity at the bone – implant interface [30,31].

The present study is limited to 6 clinical cases only, with microscopic analyses differing between the different cases due to practical issues. Nevertheless, to the authors, this is the

first time such interpositional-tissue formation at the humeral bone implant interface is observed and analyzed. This study thus represents a real confirmation that further investigations on this new interpositional-tissue have to be led. Currently, several PISA procedures have shown interesting results, up to 5 years mid-terms results on young patients (50 ± 12 years) [32]. By accurately analyzing the relationships between the PISA geometry and the nature of the interpositional-tissue nature, more personalized treatments could be developed, thus preventing from the PISA failure by reducing the number of bad diagnoses. Understanding what geometry is the most suitable for the patient is an additional step to accurately monitored the success of the PISA. In that context, numerical modelling appears as a relevant tool to define a geometry allowing for a suitable contact pressure distribution [33]. In addition, mechanobiological analyses could be performed to understand the chondrogenic power of PyC surface considering different geometries and different mechanical loadings [34–36].

5 Conclusion

In summary, cortical bone and cartilage-like tissues have been observed between the cancellous bone of the humerus and PISA. These observations witness the capacities of PISA to form and maintain an interpositional-tissue at the bone-implant interface. The properties of the interpositional-tissue probably depend on the duration of implantation, the initial diagnosis, and probably on the biomechanical conditions of the humeral bone – PyC implant - glenoid system.

6 Conflict of interests

A.Godnèche and J.Garret are participating to an receives fees for a post marker clinical follow up study initiated by Tornier SAS on this product. P.Boileau is consultant for and receives royalties from Tornier SAS. Their immediate family, and any research foundation with which they are affiliated have not received any financial payments or other benefits from any commercial entity related to the subject of this article.

7 Acknowledgements

This study was funded by Tornier SAS.

8 References

[1] F.A. Matsen, J. Clinton, J. Lynch, A. Bertelsen, M.L. Richardson, Glenoid component failure in total shoulder arthroplasty, J. Bone Jt. Surg. - Ser. A. 90 (2008) 885–896. https://doi.org/10.2106/JBJS.G.01263.

[2] A. Papadonikolakis, M.B. Neradilek, F.A. Matsen, Failure of the Glenoid Component in Anatomic Total Shoulder Arthroplasty, J. Bone Jt. Surg. 95 (2013) 2205–2212. https://doi.org/10.2106/jbjs.l.00552.

[3] W.N. Levine, C.R. Fischer, D. Nguyen, E.L. Flatow, C.S. Ahmad, L.U. Bigliani, Long-Term Follow-up of Shoulder Hemiarthroplasty for Glenohumeral Osteoarthritis, J. Bone Jt. Surg. 94 (2012) e164-1–7. https://doi.org/10.2106/JBJS.K.00603.

[4] L. Ollier, Traité des résections et des opérations conservatices que l'on peut pratiquer sur le systême osseux, Tome 2, Paris, 1988.

[5] P. Bellemère, Pyrocarbon implants for the hand and wrist, Hand Surg. Rehabil. 37 (2018) 129–154. https://doi.org/10.1016/J.HANSUR.2018.03.001.

[6] J. Garret, A. Godeneche, P. Boileau, D. Molé, M. Etzner, L. Favard, C. Levigne, F. Sirveaux, M. Gauci, C. Dezaly, G. Walch, Pyrocarbon interposition shoulder arthroplasty : preliminary results from a prospective multicenter study at 2 years of follow-up, J. Shoulder Elb. Surg. (2017) 1–9. https://doi.org/10.1016/j.jse.2017.01.002.

[7] J.J. Klawitter, J. Patton, R. More, N. Peter, E. Podnos, M. Ross, In vitro comparison of wear characteristics of PyroCarbon and metal on bone: Shoulder hemiarthroplasty, Shoulder Elb. 12 (2020) 11–22. https://doi.org/10.1177/1758573218796837.

[8] C. Cointat, J.L. Raynier, H. Vasseur, F. Lareyre, J. Raffort, M.O. Gauci, P. Boileau, Short-term outcomes and survival of pyrocarbon hemiarthroplasty in the young arthritic shoulder, J. Shoulder Elb. Surg. 31 (2022) 113–122. https://doi.org/10.1016/J.JSE.2021.06.002.

[9] C. Pangaud, J.F. Gonzalez, J.W. Galvin, M.O. Gauci, P. Boileau, Fracture of pyrocarbon humeral head resurfacing implant: a case report, J. Shoulder Elb. Surg. 29 (2020) e306–e312. https://doi.org/10.1016/j.jse.2020.02.028.

[10] P. Boileau, J.W. Galvin, C. Pangaud, J.F. Gonzalez, M.O. Gauci, Response to Letter to the Editor regarding: "Fracture of pyrocarbon humeral head resurfacing implant: a case report," J. Shoulder Elb. Surg. 30 (2021) e134–e135. https://doi.org/10.1016/j.jse.2020.11.005.

[11] R. Hudek, B. Werner, A.F. Abdelkawi, F. Gohlke, Pyrocarbon interposition shoulder arthroplasty in advanced collapse of the humeral head, Orthopade. 46 (2017) 1034–1044. https://doi.org/10.1007/s00132-017-3495-2.

[12] T. Wang, H. Li, S. Zhang, K. Li, W. Li, The effect of microstructural evolution on micromechanical behavior of pyrolytic carbon after heat treatment, Diam. Relat. Mater.

256 103 (2020) 107729. https://doi.org/10.1016/J.DIAMOND.2020.107729.

257 [13] P. Zioupos, J.D. Currey, Changes in the stiffness, strength, and toughness of human
258 cortical bone with age, Bone. 22 (1998) 57–66. https://doi.org/10.1016/S8756-
259 3282(97)00228-7.

260 [14] G.M. Marcheggiani Muccioli, G. Huri, A. Grassi, T. Roberti di Sarsina, G. Carbone, E.
261 Guerra, E.G. McFarland, M.N. Doral, M. Marcacci, S. Zaffagnini, Surgical treatment of
262 infected shoulder arthroplasty. A systematic review, Int. Orthop. 41 (2017) 823–830.
263 https://doi.org/10.1007/S00264-017-3399-0.

264 [15] H. Barret, M.O. Gauci, T. Langlais, O. van der Meijden, L. Tran, P. Boileau, Pyrocarbon
265 interposition shoulder arthroplasty in young arthritic patients: a prospective
266 observational study, J. Shoulder Elb. Surg. 29 (2020) e1–e10.
267 https://doi.org/10.1016/j.jse.2019.05.044.

268 [16] G. Walch, R. Badet, A. Boulahia, A. Khoury, Morphologic study of the glenoid in primary
269 glenohumeral osteoarthritis, J. Arthroplasty. 14 (1999) 756–760.
270 https://doi.org/10.1016/S0883-5403(99)90232-2.

271 [17] J. V. Francuski, A. Radovanović, N. Andrić, V. Krstić, D. Bogdanović, V. Hadžić, V.
272 Todorović, M.L. Macanović, S.S. Petit, S. Beck-Cormier, J. Guicheux, O. Gauthier, M.K.
273 Filipović, Age-related Changes in the Articular Cartilage of the Stifle Joint in Non-
274 working and Working German Shepherd Dogs, J. Comp. Pathol. 151 (2014) 363–374.
275 https://doi.org/10.1016a/J.JCPA.2014.09.002.

276 [18] P.J. Prendergast, R. Huiskes, K. Søballe, Biophysical stimuli on cells during tissue
277 differentiation at implant interfaces, J. Biomech. 30 (1997) 539–548.
278 https://doi.org/10.1016/S0021-9290(96)00140-6.

279 [19] R. Lugo, P. Kung, C.B. Ma, Shoulder biomechanics, Eur. J. Radiol. 68 (2008) 16–24.
280 https://doi.org/10.1016/J.EJRAD.2008.02.051.

281 [20] V.L. Popov, A.M. Poliakov, V.I. Pakhaliuk, Synovial Joints. Tribology, Regeneration,
282 Regenerative Rehabilitation and Arthroplasty, Lubricants. 9 (2021) 15.
283 https://doi.org/10.3390/lubricants9020015.

284 [21] Z. Zhao, Q. Tan, A. Jiang, S. Sun, Z. Liu, W. Li, C. Song, H. Leng, Evidence of
285 subchondral bone's effects on articular cartilage damage in OVX-OA rat, Eng. Fract.
286 Mech. 233 (2020) 107081. https://doi.org/10.1016/j.engfracmech.2020.107081.

287 [22] K. Grandfield, R.P. Herber, L. Chen, S. Djomehri, C. Tam, J.H. Lee, E. Brown, W.R.
288 Woolwine, D. Curtis, M. Ryder, J. Schuck, S. Webb, W. Landis, S.P. Ho, Strain-guided

mineralization in the bone-PDL-cementum complex of a rat periodontium, Bone Reports. 3 (2015) 20–31. https://doi.org/10.1016/j.bonr.2015.04.002.

[23] M. Benjamin, T. Kumai, S. Milz, B.M. Boszczyk, A.A. Boszczyk, J.R. Ralphs, The skeletal attachment of tendons—tendon 'entheses,' Comp. Biochem. Physiol. Part A Mol. Integr. Physiol. 133 (2002) 931–945. https://doi.org/10.1016/S1095-6433(02)00138-1.

[24] M. Benjamin, E.J. Evans, L. Copp, The histology of tendon attachments to bone in man., J. Anat. 149 (1986) 89–100. /pmc/articles/PMC1261636/?report=abstract (accessed January 26, 2022).

[25] D.P. Cury, F.J. Dias, M.A. Miglino, I.S. Watanabe, Structural and Ultrastructural Characteristics of Bone-Tendon Junction of the Calcaneal Tendon of Adult and Elderly Wistar Rats, PLoS One. 11 (2016) e0153568. https://doi.org/10.1371/JOURNAL.PONE.0153568.

[26] E. Kheir, D. Shaw, Hyaline articular cartilage, Orthop. Trauma. 23 (2009) 450–455. https://doi.org/10.1016/j.mporth.2009.01.003.

[27] D.R. Eyre, The collagens of articular cartilage, Semin. Arthritis Rheum. 21 (1991) 2–11. https://doi.org/10.1016/0049-0172(91)90035-X.

[28] Y.A. Rim, J.H. Ju, The Role of Fibrosis in Osteoarthritis Progression, Life 2021, Vol. 11, Page 3. 11 (2020) 3. https://doi.org/10.3390/LIFE11010003.

[29] P. Bhattaram, U. Chandrasekharan, The joint synovium: A critical determinant of articular cartilage fate in inflammatory joint diseases, Semin. Cell Dev. Biol. 62 (2017) 86–93. https://doi.org/10.1016/J.SEMCDB.2016.05.009.

[30] R. Gauthier, H. Follet, A.M. Trunfio-Sfarghiu, D. Farlay, N. Attik, S. Meille, J. Chevalier, D. Mitton, Osteocyte pericellular and perilacunar matrices as markers of bone–implant mechanical integrity, BIOCELL. 46 (2022) 2209–2216. https://doi.org/10.32604/biocell.2022.022290.

[31] F.A. Shah, P. Thomsen, A. Palmquist, A Review of the Impact of Implant Biomaterials on Osteocytes, J. Dent. Res. 97 (2018) 977–986. https://doi.org/10.1177/0022034518778033.

[32] J. Garret, A. Godenèche, P. Boileau, D. Molé, M. Etzner, L. Favard, C. Lévigne, F. Sirveaux, G. Walch, Midterm results of pyrocarbon interposition shoulder arthroplasty: good outcomes after posttraumatic osteonecrosis without malunion of the tuberosities, JSES Int. 6 (2022) 787–794. https://doi.org/10.1016/J.JSEINT.2022.05.007.

[33] P. Büchler, A. Farron, Benefits of an anatomical reconstruction of the humeral head during shoulder arthroplasty: A finite element analysis, Clin. Biomech. 19 (2004) 16–23. https://doi.org/10.1016/j.clinbiomech.2003.09.009.

[34] A. Hannoun, G. Ouenzerfi, L. Brizuela, S. Mebarek, C. Bougault, M. Hassler, Y. Berthier, A.M. Trunfio-Sfarghiu, Pyrocarbon versus cobalt-chromium in the context of spherical interposition implants: an in vitro study on cultured chondrocytes, Eur. Cell. Mater. 37 (2019) 1–15. https://doi.org/10.22203/eCM.v037a01.

[35] A. Impergre, A.M. Trunfio-Sfarghiu, C. Der-Loughian, L. Brizuela, S. Mebarek, B. Ter-Ovanessian, A. Bel-Brunon, Y. Berthier, B. Normand, Tribocorrosion of Polyethylene/Cobalt Contact Combined with Real-Time Fluorescence Assays on Living Macrophages: Development of A Multidisciplinary Biotribocorrosion Device, Biotribology. 18 (2019) 100091. https://doi.org/10.1016/j.biotri.2019.100091.

[36] A. Hannoun, E. Perrier-Groult, L. Cureu, M. Pasdeloup, Y. Berthier, F. Mallein-Gerin, A.M. Trunfio-Sfarghiu, New “Tribo-bioreactor” for In-situ Monitoring of the Mechanical Stress Transmission at the Cellular Level: Application to Cartilage Tissue Engineering, Biotribology. 25 (2021) 100158. https://doi.org/10.1016/j.biotri.2020.100158.